

UNCLASSIFIED

AD 274 355

*Reproduced
by the*

**ARMED SERVICES TECHNICAL INFORMATION AGENCY
ARLINGTON HALL STATION
ARLINGTON 12, VIRGINIA**

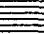


UNCLASSIFIED

NOTICE: When government or other drawings, specifications or other data are used for any purpose other than in connection with a definitely related government procurement operation, the U. S. Government thereby incurs no responsibility, nor any obligation whatsoever; and the fact that the Government may have formulated, furnished, or in any way supplied the said drawings, specifications, or other data is not to be regarded by implication or otherwise as in any manner licensing the holder or any other person or corporation, or conveying any rights or permission to manufacture, use or sell any patented invention that may in any way be related thereto.

CHINA

1. Introduction
 2. Background
 3. Methodology
 4. Results
 5. Conclusion
 6. References
 7. Appendix
 8. Index
 9. Glossary
 10. Summary
 11. Abstract
 12. Keywords
 13. Subject
 14. Topic
 15. Field
 16. Area
 17. Discipline
 18. Branch
 19. Division
 20. Department
 21. Faculty
 22. School
 23. College
 24. University
 25. Institution
 26. Organization
 27. Association
 28. Society
 29. Community
 30. Group
 31. Team
 32. Unit
 33. Section
 34. Division
 35. Department
 36. Faculty
 37. School
 38. College
 39. University
 40. Institution
 41. Organization
 42. Association
 43. Society
 44. Community
 45. Group
 46. Team
 47. Unit
 48. Section
 49. Division
 50. Department
 51. Faculty
 52. School
 53. College
 54. University
 55. Institution
 56. Organization
 57. Association
 58. Society
 59. Community
 60. Group
 61. Team
 62. Unit
 63. Section
 64. Division
 65. Department
 66. Faculty
 67. School
 68. College
 69. University
 70. Institution
 71. Organization
 72. Association
 73. Society
 74. Community
 75. Group
 76. Team
 77. Unit
 78. Section
 79. Division
 80. Department
 81. Faculty
 82. School
 83. College
 84. University
 85. Institution
 86. Organization
 87. Association
 88. Society
 89. Community
 90. Group
 91. Team
 92. Unit
 93. Section
 94. Division
 95. Department
 96. Faculty
 97. School
 98. College
 99. University
 100. Institution
 101. Organization
 102. Association
 103. Society
 104. Community
 105. Group
 106. Team
 107. Unit
 108. Section
 109. Division
 110. Department
 111. Faculty
 112. School
 113. College
 114. University
 115. Institution
 116. Organization
 117. Association
 118. Society
 119. Community
 120. Group
 121. Team
 122. Unit
 123. Section
 124. Division
 125. Department
 126. Faculty
 127. School
 128. College
 129. University
 130. Institution
 131. Organization
 132. Association
 133. Society
 134. Community
 135. Group
 136. Team
 137. Unit
 138. Section
 139. Division
 140. Department
 141. Faculty
 142. School
 143. College
 144. University
 145. Institution
 146. Organization
 147. Association
 148. Society
 149. Community
 150. Group
 151. Team
 152. Unit
 153. Section
 154. Division
 155. Department
 156. Faculty
 157. School
 158. College
 159. University
 160. Institution
 161. Organization
 162. Association
 163. Society
 164. Community
 165. Group
 166. Team
 167. Unit
 168. Section
 169. Division
 170. Department
 171. Faculty
 172. School
 173. College
 174. University
 175. Institution
 176. Organization
 177. Association
 178. Society
 179. Community
 180. Group
 181. Team
 182. Unit
 183. Section
 184. Division
 185. Department
 186. Faculty
 187. School
 188. College
 189. University
 190. Institution
 191. Organization
 192. Association
 193. Society
 194. Community
 195. Group
 196. Team
 197. Unit
 198. Section
 199. Division
 200. Department
 201. Faculty
 202. School
 203. College
 204. University
 205. Institution
 206. Organization
 207. Association
 208. Society
 209. Community
 210. Group
 211. Team
 212. Unit
 213. Section
 214. Division
 215. Department
 216. Faculty
 217. School
 218. College
 219. University
 220. Institution
 221. Organization
 222. Association
 223. Society
 224. Community
 225. Group
 226. Team
 227. Unit
 228. Section
 229. Division
 230. Department
 231. Faculty
 232. School
 233. College
 234. University
 235. Institution
 236. Organization
 237. Association
 238. Society
 239. Community
 240. Group
 241. Team
 242. Unit
 243. Section
 244. Division
 245. Department
 246. Faculty
 247. School
 248. College
 249. University
 250. Institution
 251. Organization
 252. Association
 253. Society
 254. Community
 255. Group
 256. Team
 257. Unit
 258. Section
 259. Division
 260. Department
 261. Faculty
 262. School
 263



1. The first step in the process is to identify the problem or issue that needs to be addressed. This involves gathering information and understanding the context of the situation.

2. Once the problem is identified, the next step is to define the objectives and goals of the project. This helps to clarify what needs to be achieved and provides a clear direction for the team.

3. The third step is to develop a plan or strategy to address the problem. This involves breaking down the problem into smaller, manageable tasks and determining the resources needed to complete them.

4. The fourth step is to implement the plan. This involves putting the strategy into action and monitoring progress regularly to ensure that the project is on track.

5. The final step is to evaluate the results of the project. This involves assessing the outcomes against the objectives and goals and identifying any lessons learned for future projects.

[illegible]

[Illegible handwritten notes]

[illegible]

3) by ARO, Inc.,
Tennessee)

NOTICES

Qualified requesters may obtain copies of this report from ASTIA. Orders will be expedited if placed through the librarian or other staff member designated to request and receive documents from ASTIA.

When Government drawings, specifications or other data are used for any purpose other than in connection with a definitely related Government procurement operation, the United States Government thereby incurs no responsibility nor any obligation whatsoever; and the fact that the Government may have formulated, furnished, or in any way supplied the said drawings, specifications, or other data, is not to be regarded by implication or otherwise as in any manner licensing the holder or any other person or corporation, or conveying any rights or permission to manufacture, use, or sell any patented invention that may in any way be related thereto.

INITIAL STUDY OF THE EFFECT
OF CRYOSURFACE GEOMETRY
ON CRYOPUMPING

By

J. A. Collins, Jr., J. D. Haygood, and E. S. J. Wang

Aero-Space Research, Office of D/E

ARO, Inc.

a subsidiary of Sverdrup and Parcel, Inc.

April 1962

ARO Project No. 506204

ABSTRACT

An experimental study of cryogenic pumping using several cryosurfaces in the pressure ranges of 10^{-4} and 10^{-3} mm Hg is presented. At these pressures, where the mean free path of the condensable gas is on the order of the cryosurface dimensions, it is shown that the pumping rate is no longer a constant as it is in free-molecular flow, but increases through what is termed the transition range and presumably approaches a higher constant value in the continuum flow regime. Flow in the gas kinetic, gas dynamic, and transition regimes is discussed.

Experimental results are presented showing the effects on cryopumping of the addition of fins or ribs to a cryosurface, and the effect of pumping with parallel cryosurfaces at different separations.

CONTENTS

	<u>Page</u>
ABSTRACT.	ii
NOMENCLATURE.	iv
1.0 INTRODUCTION	1
2.0 APPARATUS	2
3.0 PROCEDURE.	3
4.0 RESULTS AND DISCUSSION	4
5.0 CONCLUSIONS	9
REFERENCES	10

ILLUSTRATIONS

<u>Figure</u>		
1.	Test Equipment.	11
2.	Parallel Plate Cryosurface, 18-Fin Cylinder Cryosurface, and the 3-Fin Cylinder Cryosurface . .	12
3.	Mean Free Path for CO ₂ vs Pressure and Temperature	13
4.	Pumping Rate vs Pressure for 3-Fin Cylinder Cryosurface	14
5.	Pumping Rate vs Pressure for 18-Fin Cylinder Cryosurface	15
6.	Pumping Rate vs Pressure for Parallel Plate Cryosurfaces	16
7.	Log-Probability Plot of Transition Range for 3-Fin Cylinder Cryosurface	17
8.	Log-Probability Plot of Transition Range for the Parallel Plate and the 18-Fin Cylinder Cryosurfaces	18

NOMENCLATURE

A	Cryosurface area, cm^2
d	Molecular diameter, cm
k	Boltzman constant
M	Molecular weight, g/g-mole
p	Pressure, mm Hg
p_o	Pressure of inflowing gas, mm Hg
P. R.	Pumping rate, liters/sec
Δp	Partial pressure of condensable gas, mm Hg
R	Gas constant
T	Temperature, $^{\circ}\text{K}$
dV_o/dt	Inflow rate of condensable gas at pressure p_o , liters/sec
γ	Specific heat ratio
λ	Mean free path, cm

SUBSCRIPTS

() _{fm}	Free-molecular conditions (gas kinetic)
() _c	Continuum flow conditions (gas dynamic)
() _t	Transition range conditions

1.0 INTRODUCTION

Because the cryogenic vacuum pumping technique has been found to be practical and economical for application to large vacuum chambers (Refs. 1, 2, and 3), a study of the parameters significant to cryopumping is important. One of the most important limitations of cryopumping which can be stated a priori is that the pressure in the system must always be greater than the vapor pressure of the various condensate gases at the temperature of the cryosurface; for example, at liquid helium temperature the only noncondensable gas left in the chamber will be helium, itself. Interrelated with the temperature effect is the effect produced on cryopumping by the pressure of the system. An earlier investigation (Ref. 4) was made of the pumping rate for several gases as a function of chamber pressure. That investigation showed that in the free-molecular flow region experiment agrees with kinetic theory in that volumetric pumping speed is constant. In addition, those results indicated that the pumping speed was reduced in the pressure range where the chamber pressure approaches the vapor pressure of the condensate. The question naturally arises as to the effect on cryopumping of increasing the chamber pressure beyond that of the free-molecular flow region. No information pertaining to this effect has been published.

Fluid mechanics, in general, can be separated into the three regions: continuum, transition, and free-molecular flow. In the well-known continuum region, the intermolecular collisions are the governing physical phenomena, whereas in the free-molecular flow region the molecule-surface interactions are the governing phenomena. The transition region, however, is unique in that both intermolecular and molecule-surface collisions must be considered. To determine the flow region for a particular fluid dynamics problem, a dimensionless parameter known as the Knudsen number, K_n , is usually used. The Knudsen number is the ratio of the mean free path to a characteristic body dimension, and therefore expresses the degree of interaction between molecules. Based on the Knudsen number, the three flow regimes are arbitrarily separated into the following ranges (Ref. 5): for K_n less than 0.01, the flow is in the continuum region; for K_n between 0.01 and 10, the flow is said to be in the transition region; and for K_n greater than 10, free-molecular flow conditions prevail.

The capabilities of modern low-density wind tunnels are being expanded beyond the well-developed continuum flow regime into the region of transition flow. Removal of the mass flow and reduction of the nozzle

Manuscript released by authors February 1962.

boundary layer in the low-density tunnels by cryopumping is being contemplated (Ref. 6). Thus, it is necessary to understand cryopumping, not only in the free-molecular flow region where most space simulation chambers will operate, but also in the transition and continuum flow regimes.

This report deals with the cryopumping rates mainly in the pressure ranges where the free-molecule and transition regimes are predominant. With the use of several cryosurfaces, the effects of the transition regime on cryopumping are examined, and an effect of cryosurface geometry on cryopumping in the free-molecule regime is noted and discussed.

2.0 APPARATUS

The experiments were performed in a vacuum chamber, 20 inches in diameter and 30 inches in length (Fig. 1). The details of the chamber are the same as those previously reported (Ref. 4), with the exception that the 4-inch pumpout line and high vacuum gate valve were replaced by 6-inch components.

A set of cylindrical parallel plate cryosurfaces, 4-inches in diameter and one inch thick, and several variations of finned cryosurfaces were employed in this series of experiments. Figure 2 shows the parallel plates, the 18-fin cylinder, and the 3-fin cylinder. For the 18-fin surface, the cylinder is one inch in diameter and 3.5 inches long with fins 0.5 inch in depth and 3.5 inches long. For the 3-fin surface, the cylinder is 0.75 inch in diameter and 3.5 inches long with two sets of fins that are one inch (shown in the figure) and 0.5 inch in depth. Each set of fins was mounted on the cylinder by brazing with silver solder. All of the cryosurfaces employed a vacuum-jacketed transfer line for the purpose of limiting condensation in the chamber to the cryosurface. However, this was not entirely successful, and there was a small but not negligible deposit on the vacuum jacket adjacent to the cryosurface, caused by conduction cooling of the vacuum jacket. In most cases, this excess area amounted to approximately five percent of the total cryosurface pumping area. Fortunately, for any given configuration, the deposit area was constant so that a correction for the additional cryopumping surface could be made. A flexible, vacuum-jacketed, liquid nitrogen feed line was used with the parallel plates to allow variation of the distance between the plates.

Carbon dioxide was used as the condensable gas in these experiments, and liquid nitrogen was used as the cryogenic fluid. Commercial CO₂ was too impure for the experiments and was purified before use by a vacuum recrystallization method (Ref. 4). The purified CO₂ was then passed through a pressure regulator and a calibrated flowmeter. The flow was controlled with a metering valve and could be stopped completely with a solenoid valve located in the line at the entrance to the chamber. On entering the vacuum chamber, the CO₂ was directed against the wall of the chamber for diffusion purposes.

The instrumentation used in these experiments included an Alphatron for measuring pressures above 10^{-3} torr and an ionization gage for measuring pressures below 10^{-3} torr. Both gages were calibrated for N₂ gas, and a conversion factor of 0.633 was used to obtain CO₂ pressure. Also, four copper-constantan thermocouples, calibrated to liquid nitrogen temperature, were used in the temperature study on the 3-fin cylinder. A multipoint recorder was used to measure the thermocouple output.

3.0 PROCEDURE

Each series of experiments on the finned cryosurfaces and the parallel plate cryosurfaces was performed in the same manner. When any particular cryosurface was installed in the vacuum chamber, pump-down operation began. With the cryosurface at room temperature, the pump-down operation was continued for several hours until the chamber pressure reached approximately 5×10^{-6} torr. At this time, the liquid nitrogen flow was introduced to the cryosurface. When a steady flow of liquid nitrogen was established through the cryosurface, the cryosurface had reached approximately the temperature of liquid nitrogen.

Before actual testing was started, the cryosurface was coated with a visible deposit of CO₂ to eliminate the bare surface effect (Ref. 4). Then, with the cryosurface visibly coated with CO₂ and at liquid nitrogen temperature, the chamber was pumped down to approximately 2×10^{-7} torr, the vacuum valve was closed to isolate the mechanical pumps from the chamber, and a constant CO₂ inleakage, or flow, to the chamber was established, continued for approximately 3 minutes and shut off. The pumping rate could be calculated from the pressure data which were continuously recorded through the flow period. Prior to each test, the chamber was pumped down to the pressure range mentioned above. The total chamber pressure of each test was controlled by varying the CO₂ inleakage flow rate. Only ten such tests were made at any

one time before the cryosurface was warmed to room temperature, and the test procedure started again. This was done to eliminate excessive build-up of CO₂ frost on the cryosurface which might have caused significant changes in surface area and temperature. The data sheet of a typical test for the 18-fin cylinder is presented in the following table:

Test No.	Flow Rate, cc/sec (NTP)	CO ₂ Partial Pressure, mm Hg x 10 ⁴	Chamber Pressure, mm Hg x 10 ⁴
1	0.77	3.18	3.29
2	0.41	1.63	1.72
3	0.96	3.81	3.96
4	1.17	4.74	4.90
5	1.37	5.27	5.46
6	0.26	1.04	1.12
7	0.32	1.25	1.33
8	0.63	2.47	2.56
9	1.11	4.36	4.48
10	1.71	6.61	6.86

4.0 RESULTS AND DISCUSSION

The experimental results are presented in the form of pumping rates as a function of pressure. Based on the data similar to those listed in the above table, pumping rates for each cryosurface configuration can be calculated by the following equation:

$$P.R. = \frac{760}{\Delta p} \left(\frac{dV_o}{dt} \right)$$

where dV_o/dt is the flow rate in cc/sec (NTP) and Δp is the partial pressure of CO₂. Experimentally, the CO₂ partial pressure in the previous table is obtained in each run by observing the pressure drop in the pressure-time curve after the constant inleakage flow is stopped. This method of calculating pumping rate is discussed at length in Ref. 4.

For determining the mean free path of CO₂ in the interpretation of experimental data, the following equation, as recommended by Present (Ref. 7), is used:

$$\lambda = \frac{kT}{2p\pi d^2}$$

Figure 3 shows a plot of mean free path for carbon dioxide as a function of pressure at room temperature and at 77°K.

4.1 3-FIN CRYOSURFACES

As stated previously, two sets of 3-fin surfaces were employed. Including the base cylinder without fins, a total of three different cryosurfaces was used in this series of tests. The experimental results obtained from these cryosurfaces in terms of pumping rate versus chamber pressure are shown in Fig. 4. It should be noted that the pumping rate is given in liters per second and not in the usual liters/cm²-sec units characteristic of cryogenic pumping. The unit of area was not included in the pumping rate calculation because in several cases, as will be seen later, the actual surface actively cryopumping was not known. Since, however, this is essentially a comparison study, the units of pumping rates are of secondary importance.

In further examining Fig. 4, it can be seen that in the lower pressure range, the pumping rate in all three cases is constant within experimental error. Considering this range of pressure to be in the free-molecular flow region, the experimental data agree with kinetic theory with a capture coefficient of approximately 0.55 based on the total cryosurface area. On going to higher pressures, a region is reached where the pumping rate is no longer constant, but begins to increase with increasing pressure. This is believed to be the start of the transition range in going from the free-molecular flow to the continuum region. Curves A and B, which are the data collected on the cylinder without fins and with 0.5-inch fins, respectively, cover the transition range and appear to reach a leveling-off value of pumping rate which is considered to be approaching that of the continuum flow regime. Curve C, which represents data from the cylinder with one-inch depth fins, could not be extended to a leveling-off region where constant pumping rate would be evident. The limitation in extending experimental data into the continuum region is attributed to thermal overloading of the cryosurface, as the temperature of the fins is obtained solely by conduction from the liquid-nitrogen-cooled cylinder. Thus, at the higher pressures, which means higher flow rates of CO₂, the outward portions of the fins were subject to a thermal overload which resulted in a severe reduction in pumping rate. This overloading was observed visually and experimentally. As the flow rate was increased, the CO₂ deposit on the outer regions of the fins began to flake off. Experimentally, thermocouples were placed on the 0.5-inch fins and a temperature gradient was measured across the fins. At a CO₂ flow rate of 65 cc/sec, for example, the gradient across the fins was over 55°K, i. e., the temperature of the outer edge of the fin was above 132°K.

4.2 18-FIN CYLINDER CRYOSURFACE

The data collected for the 18-fin cylinder cryosurface in the free-molecular flow region and in the beginning of the transition region are given in Fig. 5. Again thermal overloading of the fins prevented obtaining data in the continuum range of flow.

In the free-molecular flow region, the experimental pumping rate is approximately 1850 liters/sec. This pumping rate is higher than that which can be explained by kinetic theory using the surface area of the base cylinder and lower than that using total surface area of the fins and base cylinder. It is found that if the envelope area of the 18-fin cylinder, which is the projected area of a cylinder with radius equal to fin depth plus the radius of the actual cylinder, is used, and if the capture coefficient is chosen as unity, the calculated pumping rate based on kinetic theory agrees with the experimental value.

In order to understand this envelope-area concept, comprehension of the mechanism of molecular motion near the cryosurfaces is necessary. In the free-molecular flow region, the number of molecules at ambient temperature hitting a unit area of surface also at ambient temperature per unit time can be calculated by kinetic theory, and the rate of molecules hitting the surface will be equal to the rate of molecules which are rebounding from the surface. If the surface is cold, a non-equilibrium condition would exist where some of the molecules will stick to the surface and others still bounce back. However, if the surface is replaced by an orifice, where all the molecules passing through will not return, this could be exactly the case with the 18-fin cylinder. If the orifice is then bounded by deep fins on a surface at a low enough temperature to freeze out the gas, the gas molecules undergo multiple collisions with the cold surface and most are condensed. Once the depth of the fins is sufficient to freeze out all the molecules, further increase in the depth will have no effect on the cryopumping rate. With this in mind, it is obvious that the total surface area cannot be used to calculate meaningful pumping speed per unit area. One must instead use the envelope area. When this new surface area is used, the capture coefficient of the envelope is found to be unity, that is, every molecule that passes through the hypothetical envelope area is condensed.

The use of fins or honeycomb structure on a cryosurface to increase capture probability in cryopumping will be important in the design of cryopanel. However, there appear to be two limitations. First, there is an optimum length for the fins, which is a function of the thermal conductivity of fin material and of the ratio of the separation of the fins to their depth. The second apparent limitation is the amount of non-condensable gases present in the system. In these tests, the purified

CO₂ gas contained approximately 20 parts noncondensables for every 10⁶ parts CO₂. It was observed that the frost deposit covered all of the fins down to the cylinder, and there was no visible deposit on the cylinder itself between the fins; the results indicated a capture coefficient of one. Another test (Ref. 4) was performed under the same conditions with the exception that the CO₂ contained approximately 400 parts noncondensables for every 10⁶ parts CO₂. In this case, it was observed that the visible CO₂ deposit appeared only on the tips of the fins, and the capture coefficient was calculated to be approximately 0.35. This is presumably caused by the concentration of the noncondensables in the space between the fins. The noncondensables would be prevented from escaping by the inflowing CO₂ gas, and would in turn prevent the CO₂ from reaching the bottom of the space between the fins, thus reducing the effective depth of the fins. Although there is some disagreement between this picture of the effect of noncondensables and the simple kinetic theory predictions, there is no lack of evidence for the reality of the effect itself.

4.3 PARALLEL PLATE CRYOSURFACES

Two sets of tests were performed with the parallel plate cryosurfaces: the first with the plates at one-inch separation, and the second with the plates together. The results of both tests are shown in Fig. 6. Again, the transition range between the free-molecular flow and continuum flow regimes is clearly defined for both cases in the form of an S-shaped curve. Examining the part of the curve in the lower pressure range where free-molecule conditions prevail, it can be seen that the pumping rate is approaching a constant value, approximately 2400 liters/sec for the plates separated one inch. Using a capture coefficient of one for the open area between the plates and a capture coefficient of 0.55 for the external surfaces, which is the capture coefficient obtained from the experimental data with the plates together, a theoretical pumping rate can be calculated. This theoretical pumping rate is 2465 liters/sec which is approximately equal to the experimental value obtained in the test.

This result agrees with the results obtained from the 18-fin cylinder, i. e., in both cases the open area of the cryosurface appears to have a capture coefficient of one for a very pure condensable gas in the free-molecular flow region.

4.4 TRANSITIONAL FLOW PHENOMENA

It is significant that pumping rate increases in the region above the free-molecular flow region in the cryopumping of CO₂ at liquid nitrogen temperature. The unpublished data at other laboratories did indicate on occasion that experimental cryopumping rate exceeds that based on kinetic theory $A(RT/2\pi M)^{1/2}$. Some explain this discrepancy as inaccurate experimental data, others as a directed flow effect caused by one-directional motion of molecules to the cryopanel. However, the data may be actually correct if they happen to be for the transition or continuum regions.

This increase in pumping rate eventually tapers off at higher pressures where continuum flow phenomena usually occur. It has been found experimentally that the pumping rate in the continuum flow regime will somewhat obey orifice flow theory prediction, $A(\gamma RT/M)^{1/2}$. These continuum flow phenomena in cryopumping could possibly be related to orifice flow theory, considering the case where gas molecules at the chamber pressure are flowing through an imaginary orifice or conductance restriction. Since the pressure at the cryosurface is very small in comparison to that of the system, a flow process involving adiabatic expansion towards the surface could also be realized.

If $A(\gamma RT/M)^{1/2}$ and $A(RT/2\pi M)^{1/2}$ are chosen as the two limiting pumping rates, then the transition region is defined. An interesting correlation can be obtained by plotting pumping rate in the transition region, on normal probability paper, versus the logarithm of pressure. The pumping rate is plotted as the percentage transition which is defined as:

$$\% \text{ transition} = \frac{(P.R.)_t - (P.R.)_{fm}}{(P.R.)_c - (P.R.)_{fm}} \times 100$$

Figure 7 shows the probability plot for the 3-fin cylinders, and Figure 8 shows the plot for the 18-fin cylinder and the parallel plate cryosurfaces. Although there is considerable scatter in the data, all the plots show an approximately linear relationship.

The reasons for this linear relationship are not known at present. However, it seems reasonable to assume that the pressure for 50 percent transition may be used to calculate a mean free path which should be comparable to the dimensions of the cryosurface. The symmetry of the transition region, implicit in the linear relationships shown, is intriguing. It indicates that, at least for cryopumping, the transition region is subject to quite definite rules and should be subject to theoretical analysis when sufficient data become available.

The following table gives a comparison of the cryosurface dimensions and the dimensions determined from the 50-percent transition point:

Cryosurface	Cylinder		Fin Depth or Plate Separation, in.	(P. R.) _{fm} , liters/sec	(P. R.) _c , liters/sec
	Length, in.	Diameter, in.			
3-Fin Cylinder	3.5	0.75	0	600	1150
3-Fin Cylinder	3.5	0.75	0.5	950	1800
3-Fin Cylinder	3.5	0.75	1.0	1540	2490 (est.)
18-Fin Cylinder	3.5	1.00	0.5	1850	5500 (est.)
2 Parallel Cylinders	1.0	4.00	0	1790	5300
2 Parallel Cylinders	1.0	4.00	1.0	2400	7200

Cryosurface	λ at 50% Transition, in.	(P. R.) _c /(P. R.) _{fm}	$\left(\frac{\gamma RT}{M}\right)^{\frac{1}{2}} / \left(\frac{RT}{2\pi M}\right)^{\frac{1}{2}}$
3-Fin Cylinder	0.66	1.92	2.97
3-Fin Cylinder	1.04	1.80	
3-Fin Cylinder	1.34	1.91	
18-Fin Cylinder	0.67	2.97	
2 Parallel Cylinders	5.05	2.96	
2 Parallel Cylinders	1.85	3.00	2.97

From the table it is quite obvious that although the ratio, $\sqrt{2\pi\gamma}$, is valid for estimating the increase in pumping speed for certain configurations (i. e., parallel plates), it is not valid for all configurations. Therefore, it will be necessary to study many other configurations before a generally valid relationship can be developed.

5.0 CONCLUSIONS

The study of cryopumping in the higher pressure ranges has shown a definite effect of flow regime on the pumping rate of a cryosurface. From the results obtained in the gas kinetic regime and the transition range, the following conclusions are made:

1. The addition of fins to a cryosurface can increase the pumping rate and lead to capture coefficients of nearly unity.
2. The advantage of fins is greater for pure condensable gases than for those contaminated with noncondensables.
3. The pumping rate of a cryosurface is greater in the continuum range than in the free-molecular range by factors ranging up to nearly three-fold.
4. At pressures between the continuum and free-molecular regions there is a smooth transition in the pumping rate.
5. The change of pumping rate with log-pressure in the transition range follows a Gaussian distribution.

REFERENCES

1. Carlson, D. D. and Underwood, R. H. "Design of an Aero-space Systems Environmental Chamber." AEDC-TR-61-10, July 1961.
2. Bailey, Bruce and Chuan, R. L. "Cryopumping for High Vacuum with Low Power." Transactions of the 1958 Vacuum Symposium, American Vacuum Society, October 22-24, 1958.
3. Latvala, E. K. and Wang, E. S. J. "Vacuum Pumping Methods for Space Chambers." Presented at the Second Symposium on Rocket Testing in Simulated Space and High Altitude Environments, Arnold Engineering Development Center, June 1961.
4. Wang, E. S. J., Collins, J. A., Jr., and Haygood, J. D. "General Cryopumping Study." AEDC-TN-61-114, October 1961.
5. Sentman, Lee H. "Free-Molecule Flow Theory and Its Application to the Determination of Aerodynamic Forces." LMSC-448514, October 1961.
6. MacDermott, W. N. "Preliminary Experimental Results of the Reduction of Viscous Effects in a Low-Density Supersonic Nozzle by Wall Cryopumping." AEDC-TN-61-71, October 1961.
7. Present, R. D. Kinetic Theory of Gases. McGraw-Hill Book Company, Inc., New York, 1958.



Fig. 1 Test Equipment

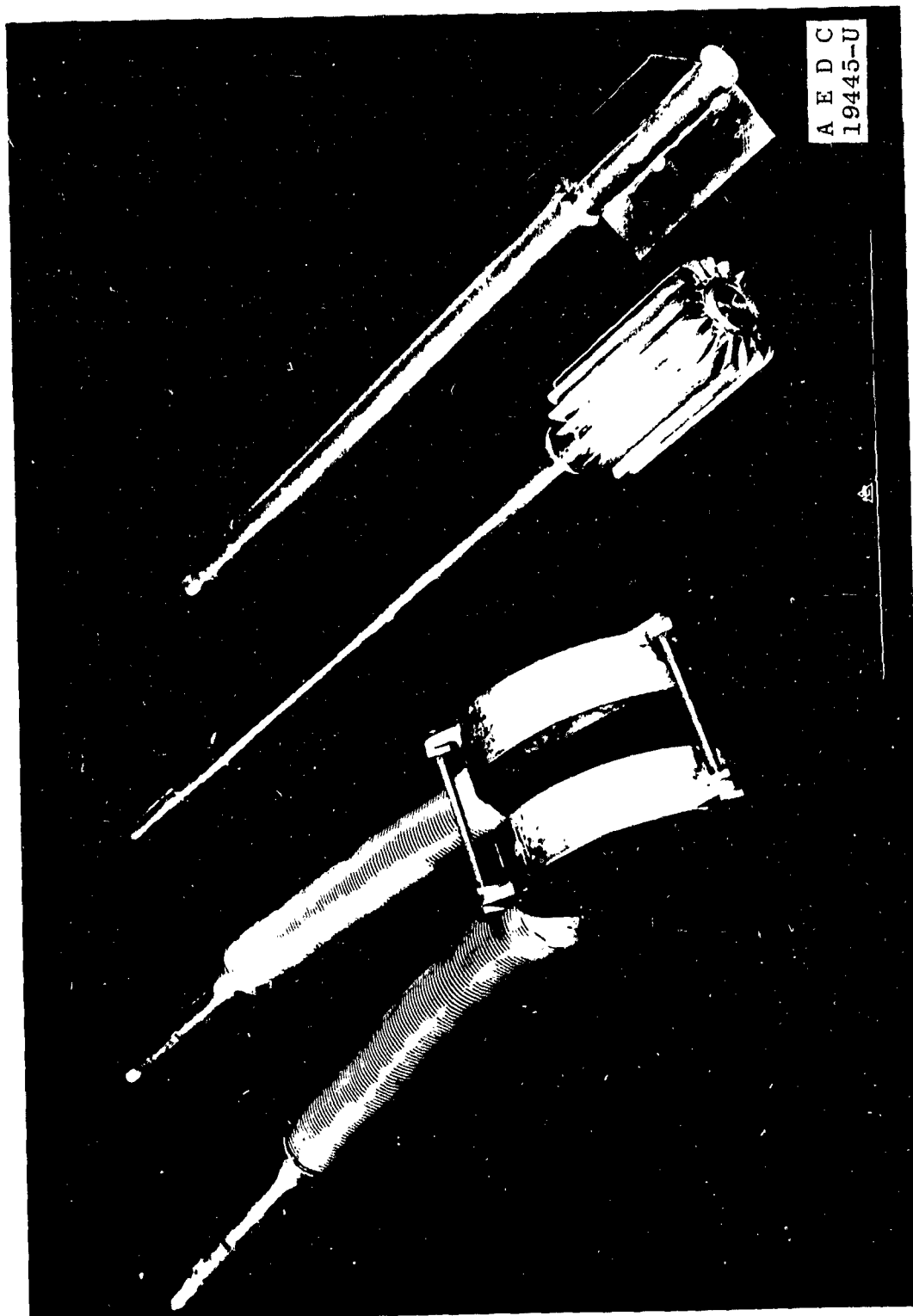


Fig. 2 Parallel Plate Cryosurface, 18-Fin Cylinder Cryosurface, and the 3-Fin Cylinder Cryosurface

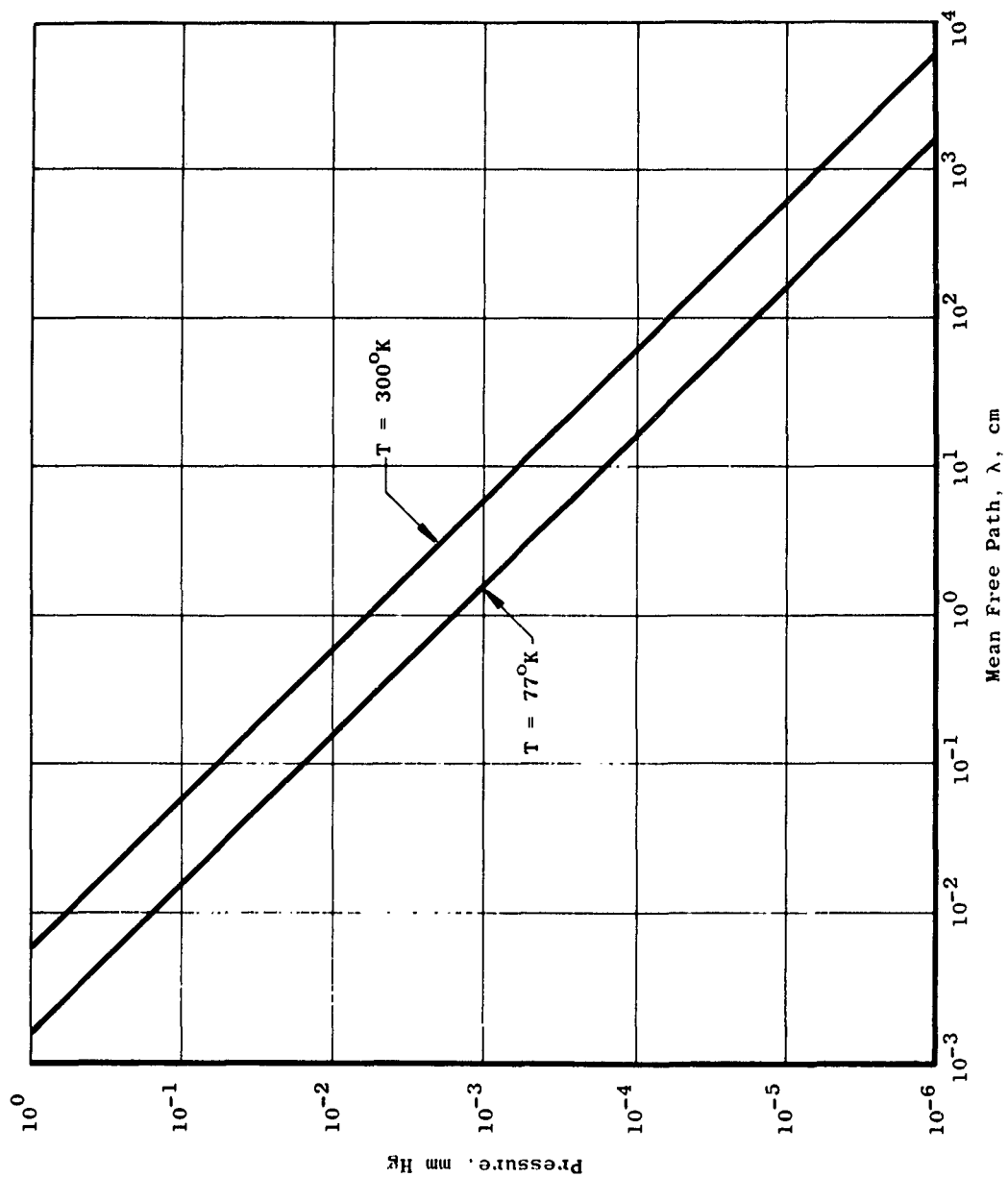


Fig. 3 Mean Free Path for CO_2 vs Pressure and Temperature

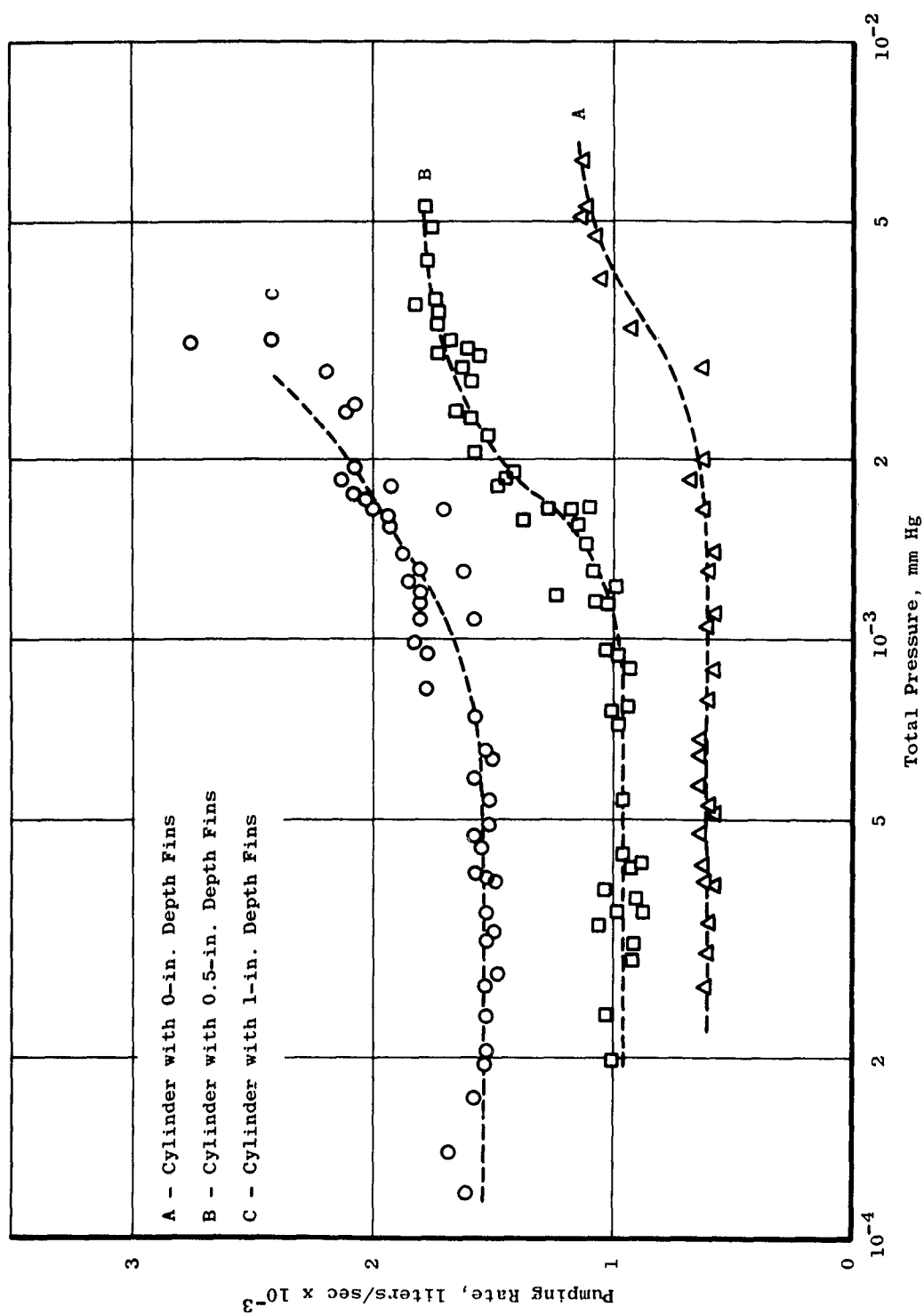


Fig. 4 Pumping Rate vs Pressure for 3-Fin Cylinder Cryosurface

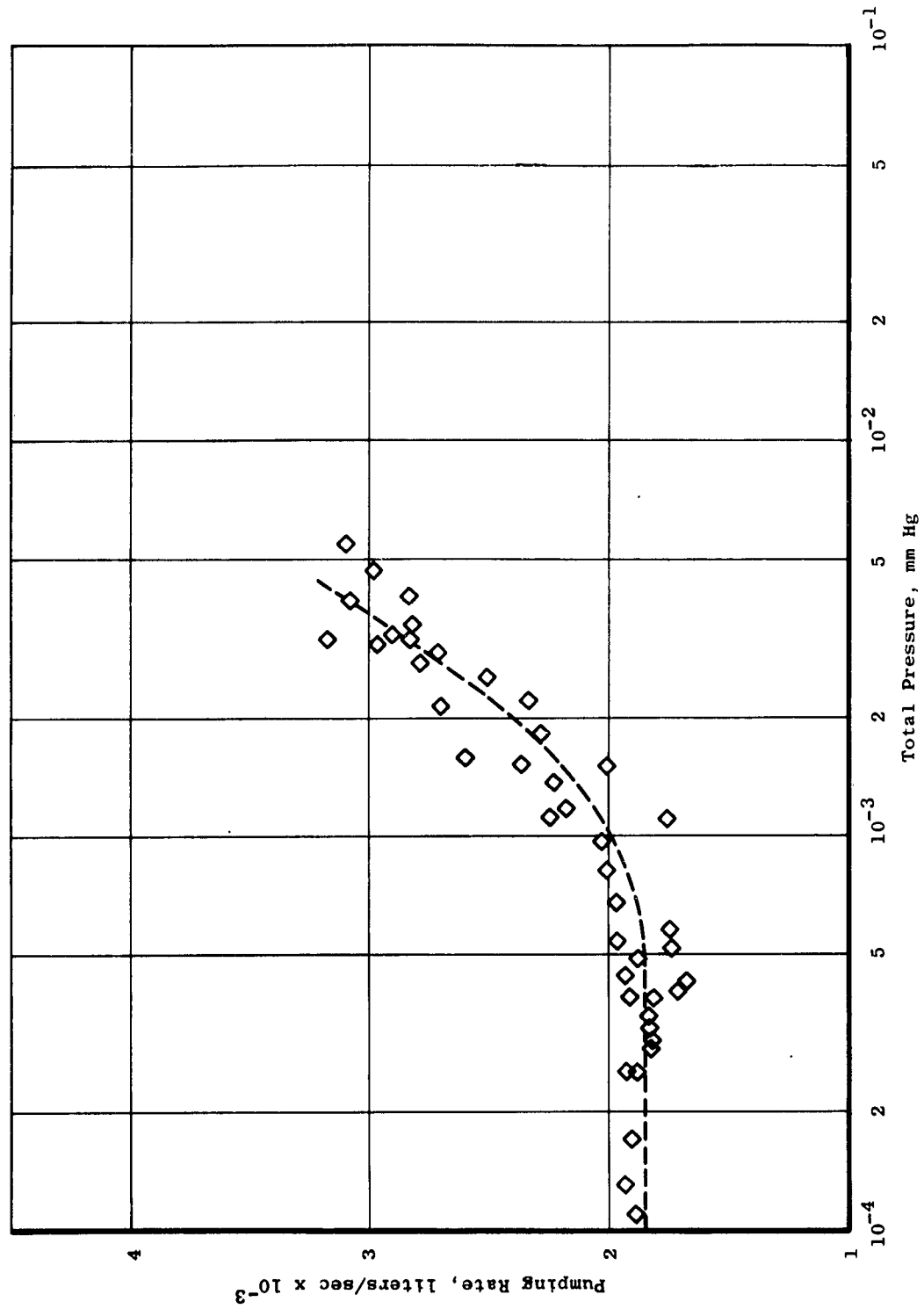


Fig. 5 Pumping Rate vs Pressure for 18-Fin Cylinder Cryosurface

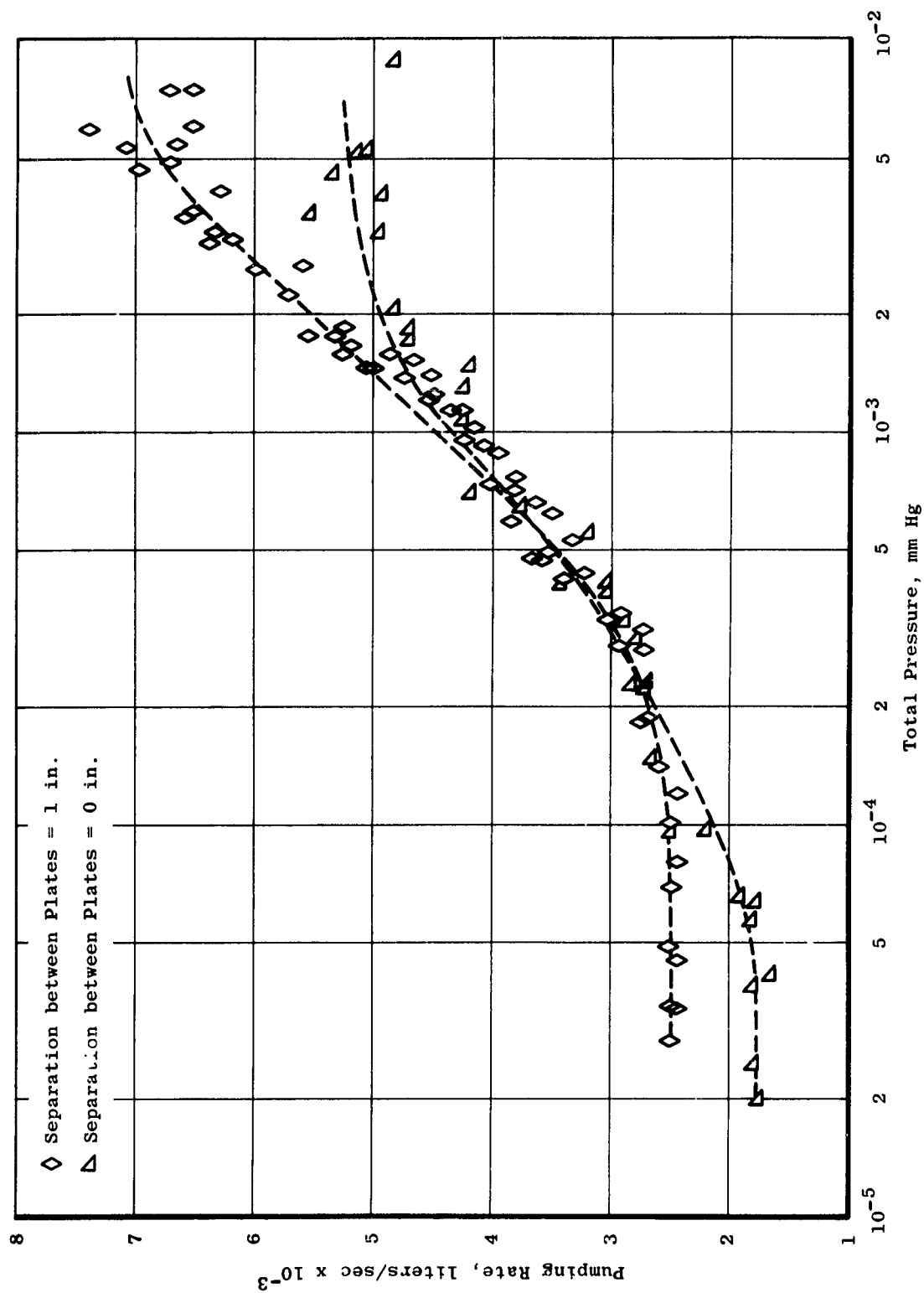


Fig. 6 Pumping Rate vs Pressure for Parallel Plate Cryosurfaces

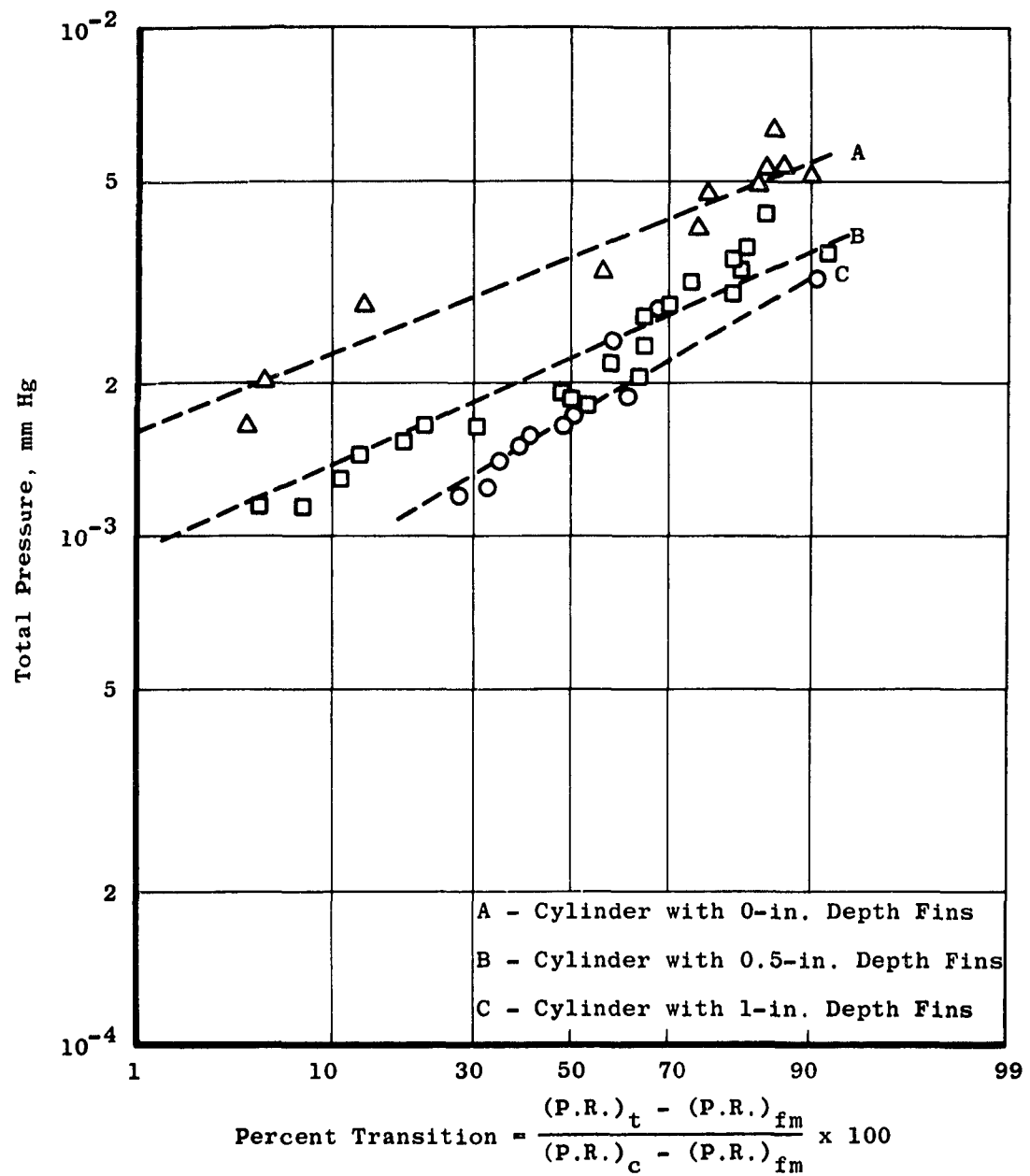


Fig. 7 Log-Probability Plot of Transition Range for 3-Fin Cylinder Cryosurface

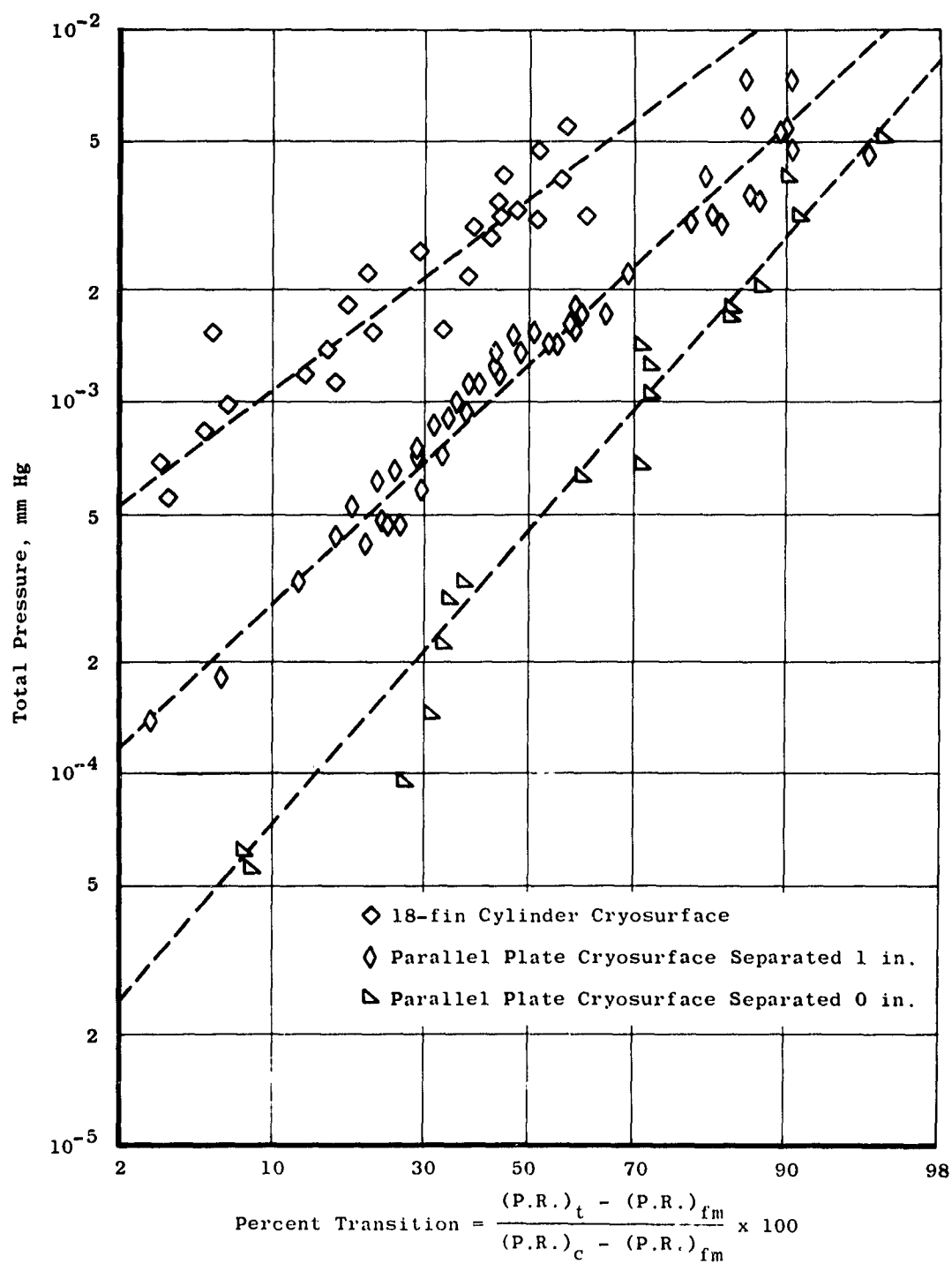


Fig. 8 Log-Probability Plot of Transition Range for the Parallel Plate and the 18-Fin Cylinder Cryosurfaces

<p>Arnold Engineering Development Center Arnold Air Force Station, Tennessee Rpt. No. AEDC-TDR-62-46. INITIAL STUDY OF THE EFFECT OF CRYOSURFACE GEOMETRY ON CRYO- PUMPING. April 1962, 22 p. incl 7 refs., illus., tables. Unclassified Report</p> <p>An experimental study of cryogenic pumping using several cryosurfaces in the pressure ranges of 10⁻⁴ and 10⁻³ mm Hg is presented. At these pressures, where the mean free path of the condensable gas is on the order of the cryosur- face dimensions, it is shown that the pumping rate is no longer a constant as it is in free-molecular flow, but in- creases through what is termed the transition range and presumably approaches a higher constant value in the con- tinuum flow regime. Flow in the gas kinetic, gas dynamic, and transition regimes is discussed. Experimental results are presented showing the effects on cryopumping of the ad- dition of fins or ribs to a cryosurface, and the effect of pumping with parallel cryosurfaces at different separations.</p>	<p>1. Cryogenics 2. Surfaces 3. Pumps 4. Vacuum systems 5. Superaerodynamics I. AFSC Program Area 806A, Project 8851, Task 88107 II. S/A 24(61-73) III. ARO, Inc., Arnold AF Sta, Tenn. IV. J. A. Collins, Jr., J. D. Haygood, E. S. J. Wang V. Available from OTS VI. In ASTIA collection</p>	<p>Arnold Engineering Development Center Arnold Air Force Station, Tennessee Rpt. No. AEDC-TDR-62-46. INITIAL STUDY OF THE EFFECT OF CRYOSURFACE GEOMETRY ON CRYO- PUMPING. April 1962, 22 p. incl 7 refs., illus., tables. Unclassified Report</p> <p>An experimental study of cryogenic pumping using several cryosurfaces in the pressure ranges of 10⁻⁴ and 10⁻³ mm Hg is presented. At these pressures, where the mean free path of the condensable gas is on the order of the cryosur- face dimensions, it is shown that the pumping rate is no longer a constant as it is in free-molecular flow, but in- creases through what is termed the transition range and presumably approaches a higher constant value in the con- tinuum flow regime. Flow in the gas kinetic, gas dynamic, and transition regimes is discussed. Experimental results are presented showing the effects on cryopumping of the ad- dition of fins or ribs to a cryosurface, and the effect of pumping with parallel cryosurfaces at different separations.</p>	<p>1. Cryogenics 2. Surfaces 3. Pumps 4. Vacuum systems 5. Superaerodynamics I. AFSC Program Area 806A, Project 8851, Task 88107 II. S/A 24(61-73) III. ARO, Inc., Arnold AF Sta, Tenn. IV. J. A. Collins, Jr., J. D. Haygood, E. S. J. Wang V. Available from OTS VI. In ASTIA collection</p>	
--	--	--	--	--